JACS
JOURNAL OF THE AMERICAN CHEMICAL SOCIETY

Article

pubs.acs.org/JACS

Mirror Images of Antimicrobial Peptides Provide Reflections on Their Functions and Amyloidogenic Properties

Conan K. Wang,* Gordon J. King, Anne C. Conibear, Mariana C. Ramos, Stephanie Chaousis, Sónia Troeira Henriques, and David J. Craik*

Institute for Molecular Bioscience, The University of Queensland, Brisbane, Queensland 4072, Australia

Supporting Information

ABSTRACT: Enantiomeric forms of BTD-2, PG-1, and PM-1 were synthesized to delineate the structure and function of these β-sheet antimicrobial peptides. Activity and lipid-binding assays confirm that these peptides act via a receptor-independent mechanism involving membrane interaction. The racemic crystal structure of BTD-2 solved at 1.45 Å revealed a novel oligomeric form of β-sheet antimicrobial peptides within the unit cell: an antiparallel trimer, which we suggest might be related to its membrane-active form. The BTD-2 oligomer extends into a larger supramolecular state that spans the crystal lattice, featuring a steric-zipper motif that is common in structures of amyloid-forming peptides. The supramolecular structure of BTD-2 thus represents a new mode of fibril-like assembly not previously observed for antimicrobial peptides, providing structural evidence linking antimicrobial and amyloid peptides.

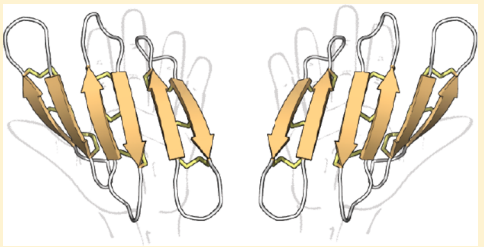

INTRODUCTION

Antimicrobial peptides have potential as next-generation therapeutics to combat the spread of drug-resistant bacteria.[1,2] Within this family are β-sheet antimicrobial peptides, of which there are around 400 members discovered so far.[3] Examples include protegrin-1 (PG-1) from porcine leukocytes[4] and polyphemusin-1 (PM-1) from horseshoe crab hemocytes,[5] as well as the θ-defensins RTD-1 and -2 from *Rhesus macaque*[6] and BTD-2 from baboon,[7] which are distinguished from other β-sheet antimicrobial peptides by their cyclic backbone (Figure 1). Recently, PG-1 was used as a starting point for the development of a potent and specific lead compound with nanomolar activity against *Pseudomonas aeruginosa*,[8] supporting the notion that antimicrobial peptides hold great promise in the future of antibiotic drug design. With a greater understanding of their mechanism of action, these peptides could attract greater interest for clinical development.[2]

Characterization of the mechanism of action of β-sheet antimicrobial peptides has largely focused on PG-1,[9−13] which is thought to act by forming pores in bacterial membranes. The discovery that PG-1 forms oligomers in solution[14] complemented by studies showing that oligomer formation is relevant to its membrane-bound state[15,16] and selectivity for bacterial cells[17] has firmly established the biological relevance of PG-1 oligomerization. However, the oligomeric structure of PG-1 is not well-established, with NMR studies providing somewhat contradictory models.[15,16] Similar to PG-1, the θ-defensins RTD-1 and BTD-2 bind lipid membranes[18,19] and probably also form pores in bacterial membranes. NMR studies have confirmed that θ-defensins oligomerize in solution;[20] but again, their oligomeric structure has remained elusive.

β-sheet antimicrobial peptides have also attracted interest because they have functional properties similar to those of amyloid peptides.[21,22] For example, PG-1 has been shown to form fibrils similar to those of disease-associated amyloids.[23,24] The link between antimicrobial peptides and amyloid peptides is still tentative but intriguing because it suggests that understanding the function and structure of β-sheet antimicrobial peptides might also lead to new approaches to treat Alzheimer's disease and other protein aggregation disorders.

Inspired by studies showing that peptide enantiomers can be used to investigate function,[25−27] here we postulated that a comparison of the activities of the naturally occurring forms of BTD-2, PG-1, and PM-1 with their enantiomeric forms would further our understanding on how these peptides are toxic to bacteria. Furthermore, given that recent crystallographic studies have revealed how amyloid peptides self-associate,[28−30] we also postulated that the crystal structures of the β-sheet antimicrobial peptides might provide new insights into their supramolecular state and therefore their mode of action. For this purpose, we determined the atomic structure of BTD-2 using an approach called racemic crystallography that uses mixtures of enantiomeric pairs to enable facile crystal formation and elucidation of high-resolution atomic structures.[31,32] The crystal structure obtained using this approach revealed a novel oligomeric form of β-sheet antimicrobial peptides, which could represent their active form and shows that they can form amyloid-like fibrils.

Received: March 9, 2016
Published: April 11, 2016

ACS Publications © 2016 American Chemical Society

DOI: 10.1021/jacs.6b02575
J. Am. Chem. Soc. 2016, 138, 5706−5713

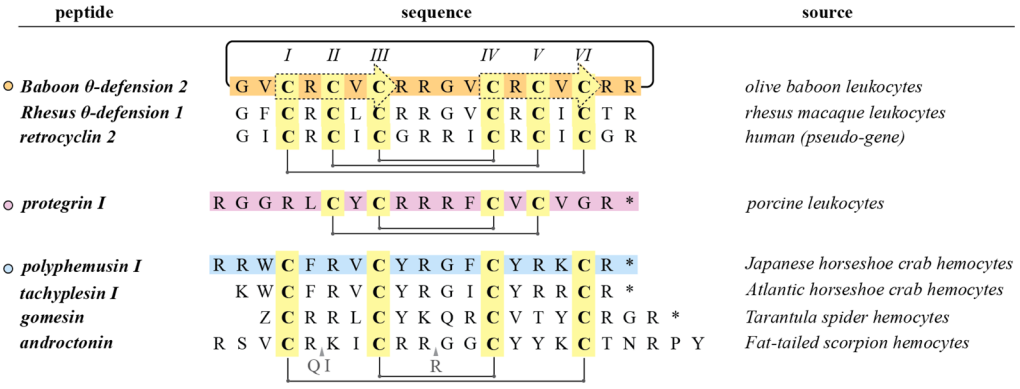

Figure 1. Selected sequences of θ-defensins and structurally related β-sheet antimicrobial peptides. The name of each peptide is shown alongside its sequence and origin. For the θ-defensins, the positions of the Cys residues are labeled using Roman numerals, and the proposed β-secondary structure and the cyclic backbone are marked using a dotted arrow. For all peptides, the disulfide bond connectivity is shown. The asterisks indicate amidated C-termini. The three peptides selected for further study in this work are baboon θ-defensin 2 (BTD-2, orange), protegrin I (PG-1, purple), and polyphemusin I (PM-1, blue).

EXPERIMENTAL PROCEDURES

Materials. Fmoc-protected amino acids, resins, and coupling agents were purchased from ChemImpex International. All other reagents were purchased from Auspep, Merck, and Sigma, and used without further purification.

Peptide Synthesis and Purification. Assembly, synthesis, purification, cyclization, and oxidation of L-BTD-2 has been described previously.[19] D-BTD-2 was synthesized and purified as described for L-BTD-2. L-PG-1, D-PG-1, L-PM-1, and D-PM-1 were synthesized using Fmoc solid-phase peptide synthesis (SPPS), as described previously.[33] Linear peptides were assembled on 2-chlorotrityl chloride (2CTC) resin. Couplings were performed using 4 equiv of Fmoc-protected amino acids, 3 equiv of HATU (*O*-(7-azabenzotriazol-1-y1)-*N*,*N*,*N*′,*N*′-tetramethyluroniumhexafluoro-phosphate) or HCTU (*O*-(1*H*-6-chlorobenzotriazol-1-y1)-*N*,*N*,*N*′,*N*′-tetramethyluronium-hexafluorophosphate), and 6 equiv of *N*,*N*-diisopropylethylamine (DIPEA) in dimethylformamide (DMF) for 2 × 10 min. Fmoc deprotection was carried out with 30% (v/v) piperidine in DMF. After each coupling and deprotection step, the resin was washed with DMF (3×), dichloromethane (DCM) (3×), and DMF (3×). Peptides were cleaved from the resin using 1% (v/v) TFA (trifluoroacetic acid) in DCM (dichloromethane).

Oxidation of L-PG-1, D-PG-1, L-PM-1, and D-PM-1 was carried out under acidic conditions with 50% (v/v) acetonitrile. Concentrated I_2 solution was added to oxidize the peptide over 20 min. Reactions were quenched with L-ascorbic acid, the reaction diluted with water (to 10% v/v acetonitrile), and immediately purified by RP-HPLC. Purity of fractions was assessed using ESI-MS and analytical HPLC. Average masses were calculated using online tools available from CyBase.[34]

Antimicrobial Assays. The antimicrobial activity of the peptides was measured by bacterial growth inhibition as described previously.[19] Briefly, the susceptibility of the Gram-negative *Escherichia coli* ATCC 25922 was studied using a microtiter broth dilution method using both Mueller Hinton Broth (MHB) with 2-fold dilutions of the peptides ranging from 0.03 to 64 μM and incubated at 37 °C for 24 h. Standard antibiotic solutions (collestin and tetracycline for *E. coli*) were also tested in concentrations ranging from 0.03 to 64 μg/mL. The minimum inhibitory concentration (MIC) was the lowest concentration showing no visible growth.

Surface Plasmon Resonance. Membrane binding studies were conducted as previously described.[19] Peptide solutions for membrane-binding studies were prepared in HEPES (10 mM, pH 7.4) containing 150 mM NaCl, and eight concentrations were tested (64, 32, 16, 8, 4, 2, 1, and 0 μM). Extracted lipids from *E. coli* (*E. coli* polar lipids extract, containing phosphatidylethanolamine/phosphatidylglycerol/cardiolipin (67:23.2:9.8 weight ratio)) were purchased from Avanti Polar Lipids. Surface plasmon resonance measurements were carried out on a Biacore 3000 instrument using an L1 sensor chip. The affinity of each peptide for the membrane was compared on the basis of the peptide to lipid ratio (P/L) obtained at a reporting point (t = 175 s) at the end of the association phase and calculated for each peptide and lipid system tested.

CD Spectroscopy. Spectra were recorded for the peptides in water at room temperature with a 0.1 cm path length quartz cell by accumulating three scans, from 190 to 260 nm using a CD spectropolarimeter (Jasco J-810). Peptides were dissolved in water at 25 μM and analyzed. Molar ellipticity (θ) was determined as previously described.[33]

NMR Spectroscopy. Peptides were dissolved in H_2O/D_2O (9:1, v/v) at a concentration of 0.5 mM. NMR spectra were recorded on a Bruker Avance-500 or Avance-600 MHz NMR spectrometer at 298 K. The mixing time was 80 and 200 ms for TOCSY and NOESY experiments, respectively. Spectra were processed using Topspin 1.2 (Bruker) and analyzed using CCPNMR 2.2.2.[35] Spectra were internally referenced to 2,2-dimethyl-2-silapentane-5-sulfonic acid (DSS) at 0.00 ppm. Secondary shifts were calculated using previously reported random coil chemical shifts.[36]

Peptide Crystallization and Data Acquisition. Lyophilized peptides (i.e., L-BTD-2 and D-BTD-2) were dissolved in water in equimolar amounts to a concentration of 2.7 mg mL^{-1}. Crystallization screening was performed at the UQ ROCX diffraction facility. Protein crystallization trials were performed in 96-well plates (commercially available Molecular Dimensions JCSG and Hampton Research Index) using the hanging drop vapor diffusion method at 20 °C. Each peptide mixture (100 nL) was mixed with crystallization solution (100 nL) using a Mosquito crystallization robot (TTP Labtech, UK), and trays were incubated and imaged in a RockImager 1000 (Formulatrix, USA).

After subsequent rounds of optimization of peptide concentration and crystallization conditions, we successfully obtained diffraction-quality crystals that grew overnight. The following condition was used to obtain crystals at 20 °C: 1 M ammonium sulfate, 15% PEG 3350, 0.1 M Bis-tris, pH 5.5. Crystals were then flash-cooled and stored in liquid nitrogen. X-ray diffraction data was collected at the Australian Synchrotron MX2 beamline at a wavelength of 0.9537 Å and recorded with an ADSC Quantum 315r detector.

Structure Determination. Crystal structures were determined using the molecular replacement method with the program PHASER. The solution structure of BTD-2 (Protein Databank ID: 2LYE) was modified in silico by truncating the Arg side chains, and the modified structure was used as the initial search model for determination of the structure of the true racemate of BTD-2. The structures were refined with rounds of manual model building in COOT[37] and refinement in PHENIX Refine,[38] as described previously.[39] Cross-validation R_{free} calculation was performed with ∼5.4% of the data. The models were validated with PROCHECK.[40] The final R_{work}/R_{free} obtained for the crystal structure of the true racemate of BTD-2 was 22.15%/25.96%.

DOI: 10.1021/jacs.6b02575
J. Am. Chem. Soc. 2016, 138, 5706−5713

For the true racemate structure of BTD-2, 95% of the L-amino acids (residues other than Gly and Pro) are within the most favored region of the Ramachandran plot, and 5% were in the additionally allowed regions. Data collection and refinement statistics are given in Supporting Table 1. The final refined models have been deposited in the Protein Data Bank with the code 5INZ.

RESULTS AND DISCUSSION

The L- and D-forms of BTD-2, PG-1, and PM-1 were synthesized and tested for activity against the Gram negative bacterium *Escherichia coli* to confirm that the synthetic peptides were antimicrobial. As shown in Table 1, the L-peptides displayed MIC values in the low micromolar range, consistent with previous reports.[5,19,41] PM-1 was more active than PG-1, which in turn was more active than BTD-2. The higher activity of PM-1 is probably due to a higher content of positively charged amino acids, i.e., arginine and lysine, and bulky hydrophobic amino acids, such as tyrosine and tryptophan, suggesting that the activity of β-sheet antimicrobial peptides can be fine-tuned by targeted mutations. Because the activities of the D-peptides were similar to that of their respective L-forms, their activity appears not to involve a chiral receptor. This suggestion is further supported by the similarities of the L-/D-mixtures and the enantiomerically pure samples.

Table 1. Antimicrobial Activity and Lipid Binding Affinity

peptide	MIC (μM)[a]
L-BTD-2	16
D-BTD-2	[8−16]
L-BTD-2/D-BTD-2 (1:1)	[8−16]
L-PG-1	[1−4]
D-PG-1	[0.25−4]
L-PG-1/D-PG-1 (1:1)	[0.25−4]
L-PM-1	[0.03−0.5]
D-PM-1	[0.03−1]
L-PM-1/D-PM-1 (1:1)	[0.25−4]

[a]Antimicrobial activity against *E. coli* ATCC25922 was determined in a microtiter assay with peptides tested in 2-fold dilution concentrations (64−0.03 μM) in MHB. MIC (minimal inhibitory concentration) is the lowest concentration of peptide showing no visible growth. When a range is provided it represents the range of MIC obtained in four replicates.

Because the current hypothesis is that these peptides act via binding to bacterial membranes,[17,19,42] we measured the binding of BTD-2, PG-1 and PM-1 to *E. coli* lipid extract using surface plasmon resonance to elucidate their membrane-binding properties. The binding affinity of various enantiomeric compositions (i.e., L-only, D-only, and L-/D-mixture) of each peptide were similar, as shown by the similar maximum amount of peptide bound to the membrane (Figure 2, top panels) and membrane-association/-dissociation kinetics (Figure 2, bottom panels). These results show that the affinity for the bacterial membrane is independent of peptide chirality and support the hypothesis that antimicrobial activity is governed by electrostatic and hydrophobic interactions with microbial membranes. It appears that direct interaction with the lipid membrane is a functional characteristic of these peptides, making them similar in this respect to antimicrobial peptides from other classes.[26,27]

To examine the role of peptide structure on activity, the structures of BTD-2, PG-1, and PM-1 in their solution state were characterized using CD and NMR (Figure 3). The CD spectra of L-PG-1 and L-PM-1 as well as the secondary Hα NMR chemical shifts confirm that they adopt the correct fold.[41,43,44] The mirror image symmetry of the D-peptide forms with their respective L-peptide forms was also confirmed using CD and NMR. Specifically, the CD spectra also showed equal but opposite rotation of each enantiomeric peptide pair, and when the D-peptide form was mixed with its respective L-peptide form in equal proportions, the circular dichroism signal of one of the forms was canceled by the other. Additionally, the chemical shifts of the D-peptide forms were essentially identical to that of their mirror image forms, confirming both enantiomeric forms to be of the same native β-sheet structure. The mirror image symmetry of each enantiomeric form shows that the structures did not affect the observed activities and supports the aforementioned hypothesis that the peptides exert their effects through direct interaction with lipid molecules of the membrane bilayer, which are generally viewed as not being enantioselective.

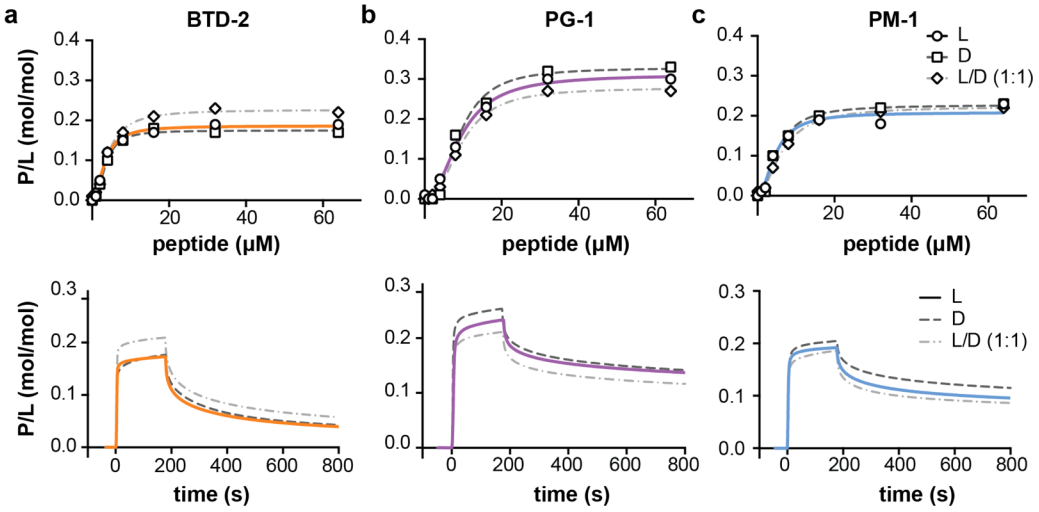

Figure 2. Binding of BTD-2, PG-1, and PM-1 to *E. coli* lipid extract. SPR was used to measure the binding of (a) BTD-2, (b) PG-1, and (c) PM-1 to model membranes composed of *E. coli* lipid extract. The top panels show the relationship between the bound peptide to lipid ratio (P/L) and the peptide concentration. The bottom panels show sensorgrams depicting the association and dissociation kinetics of binding.

DOI: 10.1021/jacs.6b02575
J. Am. Chem. Soc. 2016, 138, 5706−5713

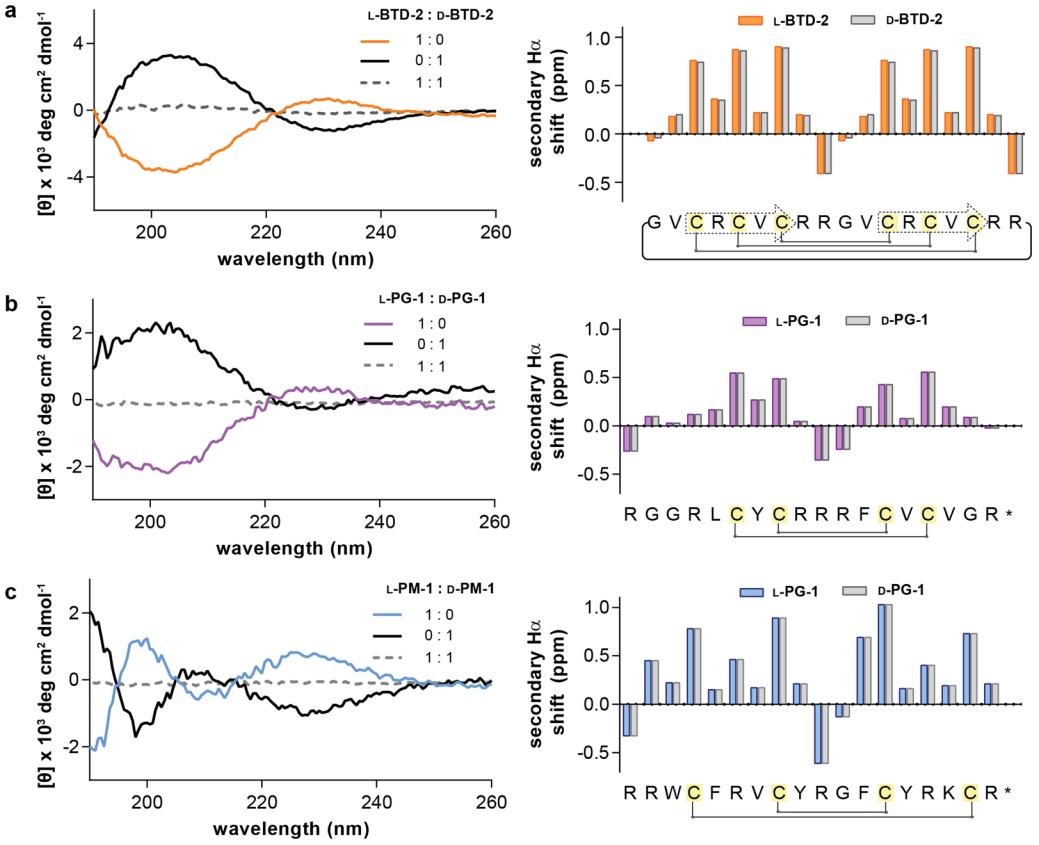

Figure 3. Solution structural information on BTD-2, PG-1, and PM-1. CD spectra (left panels) and secondary Hα chemical shifts derived using NMR (right panels) are shown for (a) BTD-2, (b) PG-1, and (c) PM-1 enantiomers. The sequence and disulfide bond connectivity of each peptide are shown underneath their respective secondary shift plot. In the case of BTD-2, the cyclic backbone is also illustrated. In the CD panel, spectra for the two enantiomers of each peptide mixed together in equal ratios are also shown.

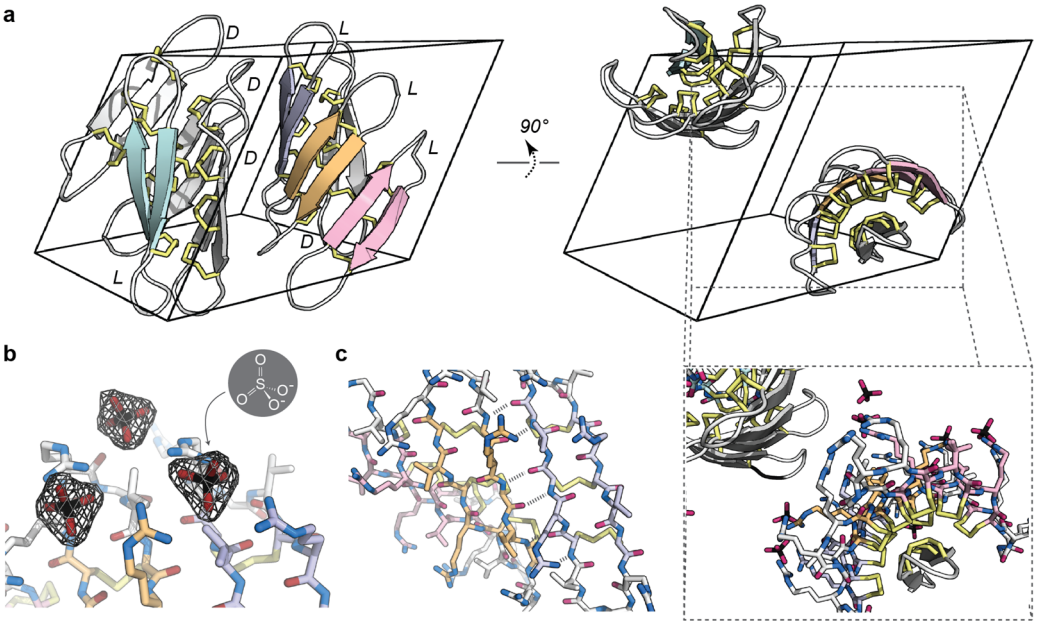

Figure 4. Racemic crystallography of BTD-2. (a) Unit cell of the true racemate in space group $P\bar{1}$ with secondary structural elements illustrated. The D-enantiomers and the L-enantiomers are labeled. The disulfide bonds are shown in yellow as stick representations. (b) $2F_o-F_c$ electron density map at a σ level of 1.0 of sulfate molecules near Arg side chains. (c) Hydrogen bond interactions between BTD-2 molecules of the same enantiomer. The peptides are shown in stick representation.

We then determined the crystal structures of the peptides using racemic crystallography, a technique used recently to crystallize recalcitrant proteins and peptides.[31] Facile crystal formation using racemic mixtures has been demonstrated for a

DOI: 10.1021/jacs.6b02575
J. Am. Chem. Soc. 2016, 138, 5706−5713

number of proteins and peptides,[45−53] and we recently demonstrated extension of the approach to elucidate the atomic resolution structures of cyclic disulfide-rich peptides.[33] Of the three peptides studied here, a racemic mixture of BTD-2 provided the best quality crystals from initial screens; however, these crystals diffracted poorly because of damage incurred during cryoprotection. Inclusion of polyethylene glycol as an additive in subsequent optimization screens eventually led to crystals that diffracted to 1.45 Å. The crystal structures were determined using the molecular replacement method and data collection, and refinement statistics are given in Supplementary Table 1.

The crystal structure of the BTD-2 racemate, shown in Figure 4, is to our knowledge the first crystal structure of a θ-defensin. It was solved in the centrosymmetric space group $P\bar{1}$, which is predicted to be the most likely space group for obtaining racemate structures of macromolecules.[54] The structure is characterized by a β-sheet that is stabilized by three disulfide bonds (Figures 4a and 5a). An overlay of the

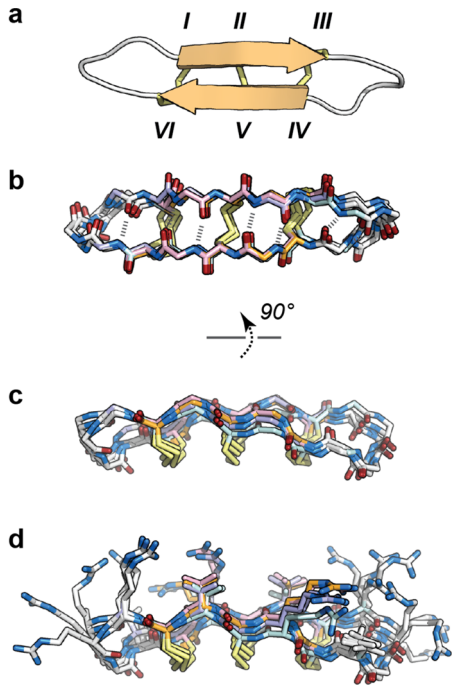

Figure 5. Structure of BTD-2 and superposition of the same enantiomers of the asymmetric unit. (a) The β-strand location as well as the disulfide bonds are shown for BTD-2. The Cys residues are labeled with Roman numerals. (b and c) Overlay of three BTD-2 molecules of the same enantiomer from the asymmetric unit with the internal hydrogen bonds indicated. (d) Different positions of the side chains are shown.

BTD-2 structures within the asymmetric unit shows there to be some flexibility in the backbone and a large degree of flexibility in the Arg side chains (Figure 5). Interestingly, the asymmetric unit contains one molecule of one enantiomeric form and three molecules of the other enantiomeric form. The enantioselectivity of molecular recognition between BTD-2 molecules provides structural evidence supporting the hypothesis that β-sheets prefer to form homochiral instead of heterochiral interactions, which until now has been based only on chemical experiments.[55] The enantioselectivity of β-sheets is attributed to the difference in contact energy between the different paired forms.[55]

The crystal structure shows the position of several sulfate ions characterized by well-resolved density that interact with the Nε and Nη protons of Arg (Figure 4b). Because sulfate ions have similar chemical properties to phosphate ions, the structural orientation of these sulfate ions with respect to nearby Arg residues suggests how BTD-2 might interact with phospholipid headgroups. It has been proposed that guanidinium−phosphate complexation is the driving force for pore formation by PG-1 and other Arg-rich antimicrobial peptides, where the cationic Arg residues interact with anionic phosphate groups as they insert into the membrane.[56] Our structural data on the interaction between Arg and anionic groups may also have implications to the function of cell-penetrating peptides, which have many cationic residues, act by binding to the membrane, and have great potential for the intracellular delivery of therapeutic molecules.[57]

Not only is the structure of BTD-2 presented here the first crystal structure of a θ-defensin, it is also the first crystal structure of a θ-defensin oligomer. Within the asymmetric unit (which was chosen to reflect the closest association between individual BTD-2 molecules), three molecules of the same enantiomeric form are held together by intermolecular hydrogen bonds forming an antiparallel arrangement (Figure 4c). We speculate that the oligomeric structure and particularly how subunits of the oligomer pack with their neighbors is relevant to the mechanism of action because previous oligomeric structures of other membrane-active peptides/proteins have also been useful for understanding function.[29,58−61] Indeed, the antiparallel arrangement of BTD-2 (Figure 6a) is comparable to the antiparallel dimer of PG-1, which has been proposed as the membrane-inserted state (Figure 6b).[16] It should be noted that an alternative oligomeric model of PG-1 has been proposed on the basis of NMR data, in which PG-1 subunits are organized parallel to their neighbors (Figure 6c).[63] Nevertheless, the oligomeric structure provides an indication on how BTD-2 molecules might be arranged in the pore and serves as a basis for future studies, using in silico methods for example.[9,10,62]

Looking beyond the asymmetric unit, we note that BTD-2 forms an elongated β-sheet that spans the crystal lattice (Figure 7a). This supramolecular assembly resembles that of an Aβ-derived peptide (Figure 7b)[28] and other amyloid-forming peptides;[30] specifically, the β-strands have an antiparallel arrangement and hydrogen bonds play a significant role in stabilizing the oligomeric structure. The similarity between the supramolecular assembly of BTD-2 and that of an Aβ-derived peptide is intriguing because it supports the provocative hypothesis that antimicrobial peptides are similar to amyloid peptides.[21,64] It has been observed that antimicrobial peptides share common biological properties with amyloid peptides.[21,22] For example, PG-1 has been shown to form fibrils similar to those of disease-associated amyloids.[23,24] Recently, we showed that BTD-2 can aggregate to form fibrils.[65] Furthermore, several amyloid proteins, including the Aβ protein, have been reported to exert strong antimicrobial activity in several common and clinically relevant microorganisms and in some cases, to exhibit antimicrobial activity exceeding that of well-known antimicrobial peptides.[66] Therefore, understanding the molecular mechanism of antimicrobial peptides might lead to new antibiotics as well as a better understanding of amyloid structure and function.

DOI: 10.1021/jacs.6b02575
J. Am. Chem. Soc. 2016, 138, 5706−5713

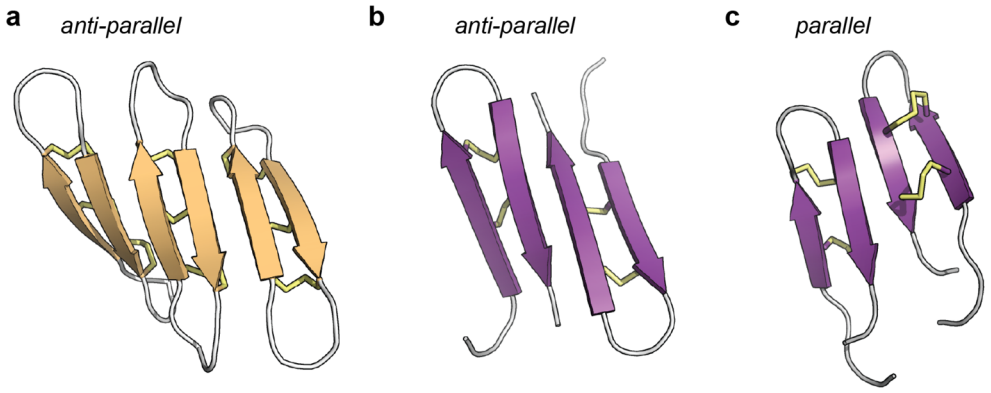

Figure 6. Oligomeric model of BTD-2 compared to oligomeric models of PG-1. (a) The racemic structure elucidated herein shows that BTD-2 forms an antiparallel oligomer, with neighboring BTD-2 molecules orientated antiparallel to one another. The trimer depicted here is observed in the chosen asymmetric unit. (b) Antiparallel[16] and (c) parallel dimer of PG-1.[63]

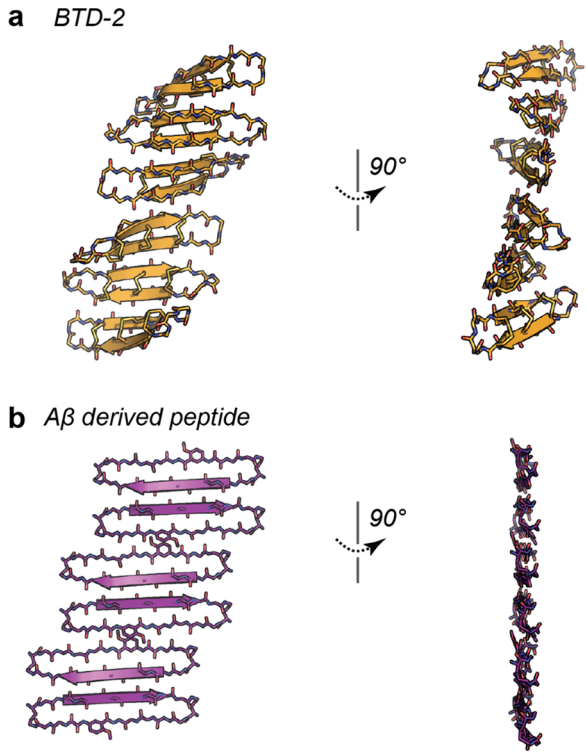

Figure 7. Assembly of hydrogen-bonded oligomers that have fibril-like properties. (a) Assembly of BTD-2 oligomers. (b) Assembly of a macrocyclic β-sheet peptide containing segments based on Aβ_{15-23} (QKLVFFAED).[28] The extended β-sheets shown in panels (a and b) run the length of the crystal lattice.

In conclusion, we have shown that the antimicrobial activity of the θ-defensin BTD-2 and related β-sheet antimicrobial peptides PG-1 and PM-1 are receptor-independent and involve membrane binding. Additionally, we present for the first time the crystal structure of an antimicrobial β-sheet peptide and a θ-defensin peptide. The structure was elucidated using racemic crystallography, further demonstrating the utility of this emerging technique for structure determination of cyclic disulfide-rich structures, which can be recalcitrant to crystallization using classical methods. Importantly, the oligomeric structure of BTD-2 provides definitive proof that antimicrobial β-sheet peptides can form antiparallel oligomers, supporting the controversial hypothesis that it is this arrangement that represents their active form, a conjecture that has up to now been derived from only NMR data. Furthermore, as the supramolecular structure is assembled into a fibril-like state that spans the crystal lattice, our structure also provides the first structural data supporting the provocative hypothesis that antimicrobial β-sheet peptides are related to amyloid-forming peptides, whose structures have recently provided valuable insights into their pathological mechanism. Because chemical synthesis using D-amino acids is becoming more accessible, we speculate that racemic crystallography will be a valuable tool in antimicrobial peptide drug discovery and may find wider applications in understanding amyloid structure.

■ ASSOCIATED CONTENT

Supporting Information

The Supporting Information is available free of charge on the ACS Publications website at DOI: 10.1021/jacs.6b02575.

Data collection and refinement statistics. (PDF)

■ AUTHOR INFORMATION

Corresponding Authors

*Tel.: 61-7-3346 2019. Fax: 61-7-3346 2101. E-mail: d.craik@imb.uq.edu.au.

*E-mail: c.wang@imb.uq.edu.au.

Notes

The authors declare no competing financial interest.

■ ACKNOWLEDGMENTS

We thank the beamline staff at the Australian Synchrotron and the University of Queensland Remote Operation Crystallization and X-ray (UQ ROCX) facility for their support. We acknowledge the facilities and the scientific and technical assistance of the Queensland NMR Network. This work was supported by grants from the Australian Research Council (DP150100443) and the National Health and Medical Research Council (NHMRC; APP1084965). C.K.W. was supported by a NHMRC Early Career Research Fellowship (546578). D.J.C. is an Australian Research Council Laureate Fellow (FL150100146). S.T.H. was supported by a Discovery Early Career Research Award (DE120103152) from the Australian Research Council. We thank Ashley Cooper for her reading of the manuscript.

DOI: 10.1021/jacs.6b02575
J. Am. Chem. Soc. 2016, 138, 5706−5713

REFERENCES

(1) Berendonk, T. U.; Manaia, C. M.; Merlin, C.; Fatta-Kassinos, D.; Cytryn, E.; Walsh, F.; Burgmann, H.; Sorum, H.; Norstrom, M.; Pons, M. N.; Kreuzinger, N.; Huovinen, P.; Stefani, S.; Schwartz, T.; Kisand, V.; Baquero, F.; Martinez, J. L. *Nat. Rev. Microbiol.* **2015**, *13*, 310−317.
(2) Fox, J. L. *Nat. Biotechnol.* **2013**, *31*, 379−382.
(3) Brogden, K. A. *Nat. Rev. Microbiol.* **2005**, *3*, 238−250.
(4) Zhao, C.; Liu, L.; Lehrer, R. I. *FEBS Lett.* **1994**, *346*, 285−288.
(5) Miyata, T.; Tokunaga, F.; Yoneya, T.; Yoshikawa, K.; Iwanaga, S.; Niwa, M.; Takao, T.; Shimonishi, Y. *J. Biochem* **1989**, *106*, 663−668.
(6) Tran, D.; Tran, P. A.; Tang, Y. Q.; Yuan, J.; Cole, T.; Selsted, M. E. *J. Biol. Chem.* **2002**, *277*, 3079−3084.
(7) Garcia, A. E.; Osapay, G.; Tran, P. A.; Yuan, J.; Selsted, M. E. *Infect. Immun.* **2008**, *76*, 5883−5891.
(8) Srinivas, N.; Jetter, P.; Ueberbacher, B. J.; Werneburg, M.; Zerbe, K.; Steinmann, J.; Van der Meijden, B.; Bernardini, F.; Lederer, A.; Dias, R. L.; Misson, P. E.; Henze, H.; Zumbrunn, J.; Gombert, F. O.; Obrecht, D.; Hunziker, P.; Schauer, S.; Ziegler, U.; Kach, A.; Eberl, L.; Riedel, K.; DeMarco, S. J.; Robinson, J. A. *Science* **2010**, *327*, 1010−1013.
(9) Lazaridis, T.; He, Y.; Prieto, L. *Biophys. J.* **2013**, *104*, 633−642.
(10) Lipkin, R. B.; Lazaridis, T. *J. Membr. Biol.* **2015**, *248*, 469−486.
(11) Hong, M.; Su, Y. *Protein Sci.* **2011**, *20*, 641−655.
(12) Su, Y.; Waring, A. J.; Ruchala, P.; Hong, M. *Biochemistry* **2011**, *50*, 2072−2083.
(13) Capone, R.; Mustata, M.; Jang, H.; Arce, F. T.; Nussinov, R.; Lal, R. *Biophys. J.* **2010**, *98*, 2644−2652.
(14) Vivcharuk, V.; Kaznessis, Y. N. *Int. J. Mol. Sci.* **2010**, *11*, 3177−3194.
(15) Mani, R.; Tang, M.; Wu, X.; Buffy, J. J.; Waring, A. J.; Sherman, M. A.; Hong, M. *Biochemistry* **2006**, *45*, 8341−8349.
(16) Roumestand, C.; Louis, V.; Aumelas, A.; Grassy, G.; Calas, B.; Chavanieu, A. *FEBS Lett.* **1998**, *421*, 263−267.
(17) Mani, R.; Cady, S. D.; Tang, M.; Waring, A. J.; Lehrer, R. I.; Hong, M. *Proc. Natl. Acad. Sci. U. S. A.* **2006**, *103*, 16242−16247.
(18) Buffy, J. J.; McCormick, M. J.; Wi, S.; Waring, A.; Lehrer, R. I.; Hong, M. *Biochemistry* **2004**, *43*, 9800−9812.
(19) Conibear, A. C.; Rosengren, K. J.; Daly, N. L.; Henriques, S. T.; Craik, D. J. *J. Biol. Chem.* **2013**, *288*, 10830−10840.
(20) Conibear, A. C.; Rosengren, K. J.; Harvey, P. J.; Craik, D. J. *Biochemistry* **2012**, *51*, 9718−9726.
(21) Kagan, B. L.; Jang, H.; Capone, R.; Teran Arce, F.; Ramachandran, S.; Lal, R.; Nussinov, R. *Mol. Pharmaceutics* **2012**, *9*, 708−717.
(22) Last, N. B.; Miranker, A. D. *Proc. Natl. Acad. Sci. U. S. A.* **2013**, *110*, 6382−6387.
(23) Jang, H.; Arce, F. T.; Mustata, M.; Ramachandran, S.; Capone, R.; Nussinov, R.; Lal, R. *Biophys. J.* **2011**, *100*, 1775−1783.
(24) Jang, H.; Ma, B.; Lal, R.; Nussinov, R. *Biophys. J.* **2008**, *95*, 4631−4642.
(25) Marelli, U. K.; Bezencon, J.; Puig, E.; Ernst, B.; Kessler, H. *Chem. - Eur. J.* **2015**, *21*, 8023−8027.
(26) Wade, D.; Boman, A.; Wahlin, B.; Drain, C. M.; Andreu, D.; Boman, H. G.; Merrifield, R. B. *Proc. Natl. Acad. Sci. U. S. A.* **1990**, *87*, 4761−4765.
(27) Wei, G.; de Leeuw, E.; Pazgier, M.; Yuan, W.; Zou, G.; Wang, J.; Ericksen, B.; Lu, W. Y.; Lehrer, R. I.; Lu, W. *J. Biol. Chem.* **2009**, *284*, 29180−29192.
(28) Pham, J. D.; Spencer, R. K.; Chen, K. H.; Nowick, J. S. *J. Am. Chem. Soc.* **2014**, *136*, 12682−12690.
(29) Pham, J. D.; Chim, N.; Goulding, C. W.; Nowick, J. S. *J. Am. Chem. Soc.* **2013**, *135*, 12460−12467.
(30) Sawaya, M. R.; Sambashivan, S.; Nelson, R.; Ivanova, M. I.; Sievers, S. A.; Apostol, M. I.; Thompson, M. J.; Balbirnie, M.; Wiltzius, J. J.; McFarlane, H. T.; Madsen, A. O.; Riekel, C.; Eisenberg, D. *Nature* **2007**, *447*, 453−457.
(31) Yeates, T. O.; Kent, S. B. *Annu. Rev. Biophys.* **2012**, *41*, 41−61.
(32) Kent, S.; Sohma, Y.; Liu, S.; Bang, D.; Pentelute, B.; Mandal, K. *J. Pept. Sci.* **2012**, *18*, 428−436.
(33) Wang, C. K.; King, G. J.; Northfield, S. E.; Ojeda, P. G.; Craik, D. J. *Angew. Chem., Int. Ed.* **2014**, *53*, 11236−11241.
(34) Wang, C. K.; Kaas, Q.; Chiche, L.; Craik, D. J. *Nucleic Acids Res.* **2007**, *36*, D206−D210.
(35) Skinner, S. P.; Goult, B. T.; Fogh, R. H.; Boucher, W.; Stevens, T. J.; Laue, E. D.; Vuister, G. W. *Acta Crystallogr., Sect. D: Biol. Crystallogr.* **2015**, *71*, 154−161.
(36) Wishart, D. S.; Bigam, C. G.; Holm, A.; Hodges, R. S.; Sykes, B. D. *J. Biomol. NMR* **1995**, *5*, 67−81.
(37) Emsley, P.; Lohkamp, B.; Scott, W. G.; Cowtan, K. *Acta Crystallogr., Sect. D: Biol. Crystallogr.* **2010**, *66*, 486−501.
(38) Afonine, P. V.; Grosse-Kunstleve, R. W.; Echols, N.; Headd, J. J.; Moriarty, N. W.; Mustyakimov, M.; Terwilliger, T. C.; Urzhumtsev, A.; Zwart, P. H.; Adams, P. D. *Acta Crystallogr., Sect. D: Biol. Crystallogr.* **2012**, *68*, 352−367.
(39) Weeratunga, S. K.; Osman, A.; Hu, N. J.; Wang, C. K.; Mason, L.; Svard, S.; Hope, G.; Jones, M. K.; Hofmann, A. *J. Mol. Biol.* **2012**, *423*, 169−181.
(40) Laskowski, R. A.; Rullmann, J. A. C.; MacArthur, M. W.; Kaptein, R.; Thornton, J. M. *J. Biomol. NMR* **1996**, *8*, 477−486.
(41) Harwig, S. S.; Waring, A.; Yang, H. J.; Cho, Y.; Tan, L.; Lehrer, R. I. *Eur. J. Biochem.* **1996**, *240*, 352−357.
(42) Zhang, L.; Scott, M. G.; Yan, H.; Mayer, L. D.; Hancock, R. E. *Biochemistry* **2000**, *39*, 14504−14514.
(43) Powers, J. P.; Rozek, A.; Hancock, R. E. *Biochim. Biophys. Acta, Proteins Proteomics* **2004**, *1698*, 239−250.
(44) Aumelas, A.; Mangoni, M.; Roumestand, C.; Chiche, L.; Despaux, E.; Grassy, G.; Calas, B.; Chavanieu, A. *Eur. J. Biochem.* **1996**, *237*, 575−583.
(45) Dang, B.; Kubota, T.; Mandal, K.; Bezanilla, F.; Kent, S. B. *J. Am. Chem. Soc.* **2013**, *135*, 11911−11919.
(46) Okamoto, R.; Mandal, K.; Sawaya, M. R.; Kajihara, Y.; Yeates, T. O.; Kent, S. B. *Angew. Chem., Int. Ed.* **2014**, *53*, 5194−5198.
(47) Avital-Shmilovici, M.; Mandal, K.; Gates, Z. P.; Phillips, N. B.; Weiss, M. A.; Kent, S. B. *J. Am. Chem. Soc.* **2013**, *135*, 3173−3185.
(48) Bunker, R. D.; Mandal, K.; Bashiri, G.; Chaston, J. J.; Pentelute, B. L.; Lott, J. S.; Kent, S. B.; Baker, E. N. *Proc. Natl. Acad. Sci. U. S. A.* **2015**, *112*, 4310−4315.
(49) Mandal, K.; Uppalapati, M.; Ault-Riche, D.; Kenney, J.; Lowitz, J.; Sidhu, S. S.; Kent, S. B. *Proc. Natl. Acad. Sci. U. S. A.* **2012**, *109*, 14779−14784.
(50) Mandal, K.; Pentelute, B. L.; Tereshko, V.; Thammavongsa, V.; Schneewind, O.; Kossiakoff, A. A.; Kent, S. B. *Protein Sci.* **2009**, *18*, 1146−1154.
(51) Banigan, J. R.; Mandal, K.; Sawaya, M. R.; Thammavongsa, V.; Hendrickx, A. P.; Schneewind, O.; Yeates, T. O.; Kent, S. B. *Protein Sci.* **2010**, *19*, 1840−1849.
(52) Pentelute, B. L.; Mandal, K.; Gates, Z. P.; Sawaya, M. R.; Yeates, T. O.; Kent, S. B. *Chem. Commun. (Cambridge, U. K.)* **2009**, *46*, 8174−8176.
(53) Pentelute, B. L.; Gates, Z. P.; Tereshko, V.; Dashnau, J. L.; Vanderkooi, J. M.; Kossiakoff, A. A.; Kent, S. B. *J. Am. Chem. Soc.* **2008**, *130*, 9695−9701.
(54) Wukovitz, S. W.; Yeates, T. O. *Nat. Struct. Biol.* **1995**, *2*, 1062−1067.
(55) Chung, D. M.; Nowick, J. S. *J. Am. Chem. Soc.* **2004**, *126*, 3062−3063.
(56) Tang, M.; Waring, A. J.; Hong, M. *J. Am. Chem. Soc.* **2007**, *129*, 11438−11446.
(57) Su, Y.; Li, S.; Hong, M. *Amino Acids* **2013**, *44*, 821−833.
(58) Hayouka, Z.; Thomas, N. C.; Mortenson, D. E.; Satyshur, K. A.; Weisblum, B.; Forest, K. T.; Gellman, S. H. *J. Am. Chem. Soc.* **2015**, *137*, 11884−11887.
(59) Ahn, V. E.; Faull, K. F.; Whitelegge, J. P.; Fluharty, A. L.; Prive, G. G. *Proc. Natl. Acad. Sci. U. S. A.* **2003**, *100*, 38−43.
(60) Wang, C. K.; Simon, A.; Jessen, C. M.; Oliveira, C. L.; Mack, L.; Braunewell, K. H.; Ames, J. B.; Pedersen, J. S.; Hofmann, A. *PLoS One* **2011**, *6*, e26793.

DOI: 10.1021/jacs.6b02575
J. Am. Chem. Soc. 2016, 138, 5706−5713

(61) Sahl, H. G.; Pag, U.; Bonness, S.; Wagner, S.; Antcheva, N.; Tossi, A. *J. Leukocyte Biol.* **2004**, *77*, 466−475.
(62) Weber, D. K.; Yao, S.; Rojko, N.; Anderluh, G.; Lybrand, T. P.; Downton, M. T.; Wagner, J.; Separovic, F. *Biophys. J.* **2015**, *108*, 1987−1996.
(63) Mani, R.; Waring, A. J.; Lehrer, R. I.; Hong, M. *Biochim. Biophys. Acta, Biomembr.* **2005**, *1716*, 11−18.
(64) Zhang, M.; Zhao, J.; Zheng, J. *Soft Matter* **2014**, *10*, 7425−7451.
(65) Wang, C. K.; Northfield, S. E.; Huang, Y. H.; Ramos, M. C.; Craik, D. J. *Eur. J. Med. Chem.* **2016**, *109*, 342−349.
(66) Soscia, S. J.; Kirby, J. E.; Washicosky, K. J.; Tucker, S. M.; Ingelsson, M.; Hyman, B.; Burton, M. A.; Goldstein, L. E.; Duong, S.; Tanzi, R. E.; Moir, R. D. *PLoS One* **2010**, *5*, e9505.

DOI: 10.1021/jacs.6b02575
J. Am. Chem. Soc. 2016, 138, 5706−5713